Journal of the American Ceramic Society

RESEARCH ARTICLE OPEN ACCESS

Investigations on the Wettability of Silicate Glass Melts on Tantalum, Niobium, and Their Oxides

Pawel Engelmann | Christian Roos

RWTH Aachen University, Aachen, Germany

Correspondence: Pawel Engelmann (pawel.engelmann@rwth-aachen.de)

Received: 10 March 2026 | **Revised:** 4 May 2026 | **Accepted:** 12 May 2026

Keywords: glass-metal contact | glass-oxide contact | niobates | niobium oxide | niobium | sticking | tantalates | tantalum oxide | tantalum | wetting

ABSTRACT

In the past, niobium and tantalum oxides were primarily investigated for potential applications in advanced optics, electronics, and photonics due to their unique physical properties. In recent heating microscopy experiments, we observed interesting wetting characteristics of silicate glass melts in contact with these materials: unlike other metals, such as copper, iron, or nickel, niobium and tantalum were hardly wetted in an oxidizing atmosphere. Likewise, sintered Nb_2O_5 and Ta_2O_5 substrates exhibited contact angles of about 130° at 1000°C. This strongly contrasts with the generally good wettability of metal oxides by oxidic melts. Interface analysis using x-ray diffraction and scanning electron microscopy revealed the formation of different sodium niobates and tantalates. Some of these phases were successfully synthesized by the mixed oxide route and likewise showed non-wetting. Especially the formation of tungsten tetragonal bronze-like phases at the interface seems to promote non-wetting, while the appearance of perovskite structures was associated with enhanced wettability. These findings are especially important because the respective phases may form a novel class of glass contact materials with potential use in glass forming.

1 | Introduction

Tantalum (Ta) and niobium (Nb) are closely related transition metals, exhibiting high melting temperatures, high corrosion resistance, and a strong affinity for oxygen. Both metals form different oxides, the most common ones being the pentoxides Ta_2O_5 and Nb_2O_5. These oxides attracted sustained research interest due to their unique combination of electrical, optical, and structural properties. Early studies focused on optical and photovoltaic applications arising from their high refractive index. Ta_2O_5 and Nb_2O_5 thin films and coatings were investigated as anti-reflection layers and optical filters [1]. Further studies focused on its high dielectric constant and wide band gap, allowing the development of dielectric layers [2, 3]. More recent work has also addressed potential medical applications [4–8].

Both oxides react with alkali and alkaline earth metal oxides and form different tantalates and niobates, the most studied systems being Ta_2O_5–Na_2O [9] and Nb_2O_5–Na_2O [10]. In both binary systems, intermediate compounds with a molar ratio of 1:2 ($Na_2Ta_4O_{11}$ and $Na_2Nb_4O_{11}$) as well as 1:1 ($NaTaO_3$ and $NaNbO_3$) exist. Moreover, non-stoichiometric solid solutions with a molar ratio of around 1:4 to 1:3 can be formed at high temperatures and once formed, persist metastably at room temperature [9, 10].

Both $NaNbO_3$ and $NaTaO_3$ show various polymorphs at different temperatures, and the structures and transformation temperatures were discussed in the literature before [11–13]. The high-temperature polymorphs for both phases form somewhat above 630°C and show a $Pm\bar{3}m$ structure. For $Ta_2Nb_4O_{11}$, the structure was reported to be $R\bar{3}c$ [14], while $Na_2Nb_4O_{11}$ undergoes a structural change at around 107°C from C2/c to $R\bar{3}c$ [15].

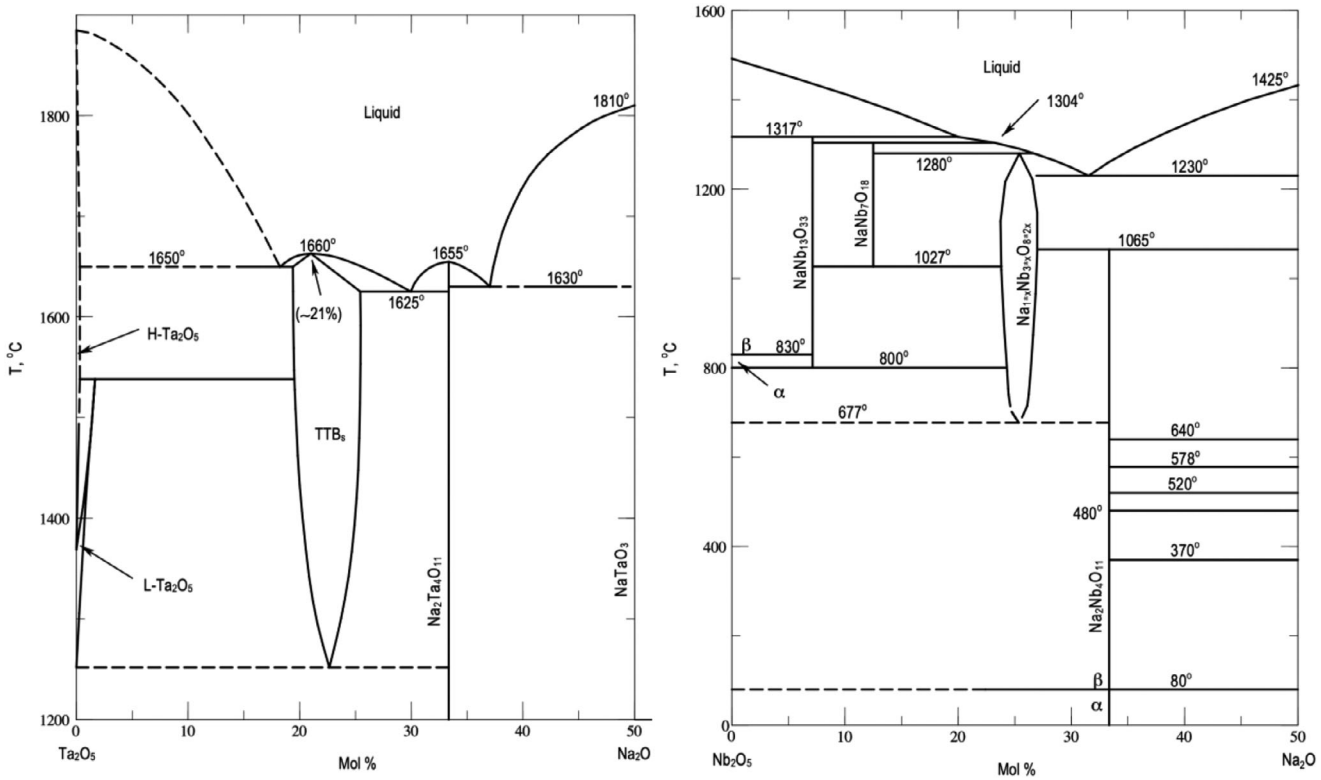

FIGURE 1 | Phase diagrams of the binary systems Ta_2O_5–Na_2O, adapted from [9], and Nb_2O_5–Na_2O, adapted from [10].

TABLE 1 | Silhouette images of different oxides being wetted by a DGG X glass melt, taken during a heating microscopy trial after isothermal dwell time for 3 h at 1000°C.

Al_2O_3	CeO_2	MgO	TiO_2	ZrO_2
				

The solid solutions show a tetragonal tungsten bronze (TTB) type substructure and an orthorhombic superstructure [16]. A lamellar oxide, $NaNb_3O_8$, was synthesized by ion exchange reaction and subsequent thermolysis from the protonic niobate $HNb_3O_8 \bullet H_2O$; however, an irreversible structural transition to the TTB phase takes place at 780°C [17]. Figure 1 shows both binary systems Na_2O–Ta_2O_5 and Na_2O–Nb_2O_5 in the composition range $\leq$ 50 mol% Na_2O.

To the best of the authors' knowledge, no investigations on the wettability of soda lime silicate glasses on tantalum or niobium oxide and tantalates or niobates exist in the literature. In general, oxides are known to be wetted well by silicate glass melts. Several oxides, such as Al_2O_3, ZrO_2, MgO, TiO_2, or CeO_2, were investigated by the authors in the same setup as used in this work (see Figure 2) in the past. All these soda lime silicate glasses showed low contact angles $\theta \lesssim 25°$ (see Table 1).

2 | Experimental

The wettability of soda–lime–silica glass on tantalum, niobium, their oxides, and various tantalates and niobates was investigated by means of heating microscopy. All experiments were carried out with the standard soda–lime–silica glass DGG X distributed by the Deutsche Glastechnische Gesellschaft (DGG). The composition of the glass determined in a round robin test can be found in Table 2. For the thermo-optical trials, glass cubes with an edge length of 3 mm were prepared from the as-delivered glass block.

Thermo-optical trials were done in a heating microscope EM301 (Hesse Instruments). The setup is shown in Figure 2. The substrate with the glass cube on top was placed on an alumina spacer and inserted into the furnace. The glass-substrate combination could then be heated up to the desired temperature.

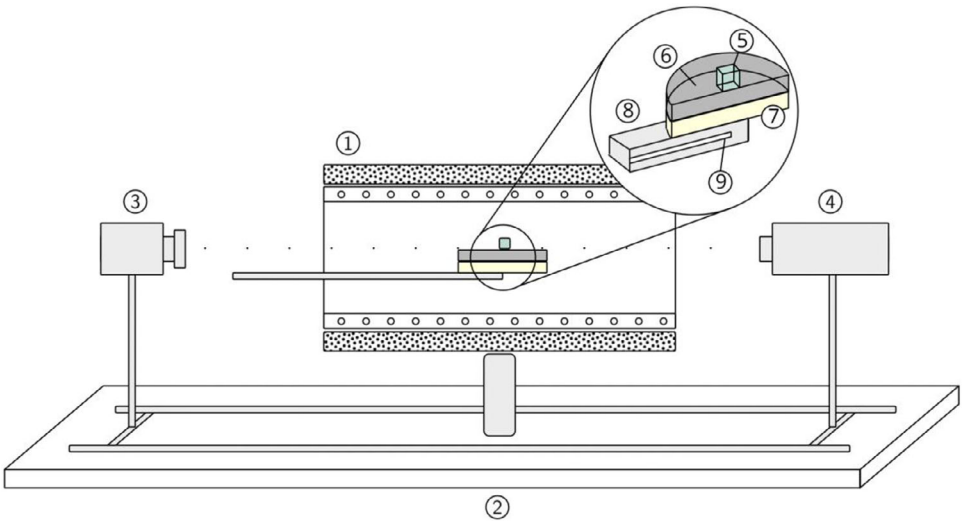

FIGURE 2 | Sketch of the heating microscopy setup: An electrically heated tube furnace (1) is located on an optical bench (2) between a light source (3) and a CCD camera with a macro lens (4). The glass cube (5) and the substrate (6) are placed on an alumina spacer (7) and mounted on the sample holder (8). A thermocouple type S (Pt-PtRh10) inside the sample holder measures the sample temperature (9).

TABLE 2 | Composition of the standard glass DGG X.

Oxide	SiO_2	Na_2O	CaO	MgO	Al_2O_3	K_2O	Fe_2O_3	SO_3	TiO_2
Mass fraction (%)	71.49	15.13	6.78	4.14	1.21	0.37	0.19	0.42	0.13

2.1 | Metallic Tantalum and Niobium

The initial trials were conducted with the metallic substrates. A tantalum rod (99.95%, metals basis) and a niobium rod (99.8%, metals basis) with a diameter of 12.7 mm were used and cut into approx. 1 mm thick slices. The substrates were then ground on silicon carbide paper up to 1200 grit and polished with diamond abrasive up to 1 μm. The thermo-optical trials were done in air and in an inert nitrogen atmosphere, respectively. The samples were heated up at a rate of 2 K/min up to 1200°C. Silhouette pictures were taken starting at 800°C during the heating process.

2.2 | Tantalum and Niobium Oxides

Due to the severe oxidation that occurred during the experiments in air, it was decided to also investigate oxide bulk substrates. Ta_2O_5 and Nb_2O_5 substrates prepared by slip casting and subsequent sintering were cut to square substrates with about 12 mm edge length. The substrates were ground on diamond plates up to 600 grit and polished with diamond abrasive up to 1 μm. The substrates were then investigated up to 1400°C or reaching the flow point at a rate of 10 K/min in the heating microscope.

2.3 | Niobates and Tantalates

A total of six different niobates and tantalates were investigated in the binary systems Na_2O–M_2O_5 (M = Ta_2O_5, Nb_2O_5). The investigated compounds can be found in Table 3. The tetragonal tungsten bronze (TTB) like tantalate phase was prepared and investigated with 22.5 mol% Na_2O.

TABLE 3 | Investigated tantalates and niobates.

System	Investigated compounds		
Na_2O–Nb_2O_5	$NaNbO_3$	$Na_2Nb_4O_{11}$	$NaNb_3O_8$
Na_2O–Ta_2O_5	$NaTaO_3$	$Na_2Ta_4O_{11}$	TTB

The synthesis of the phases was done by the established mixed-oxide route. Soda (Na_2CO_3), niobium oxide (Nb_2O_5), and tantalum oxide (Ta_2O_5) were used as raw materials, weighed according to the compositions in Table 3, and filled into cylindrical PP containers. Yttria stabilized zirconia (YSZ) milling balls and isopropyl alcohol were added, and a wet milling for 24 h on a roller bench was followed. After this homogenization process, the milling media were separated, and the slurry was evaporated overnight at approx. 80°C. The dried cake was then manually ground in a mortar, and the powder was calcined at around 850°C. The calcined material was milled and dried under the same conditions as in the homogenization process. The powder was compressed at 115 MPa into tablets with a diameter of 14 mm and a height of approx. 2 mm using a pneumatic uniaxial press. The tablets were subsequently sintered at temperatures between 1000°C and 1400°C.

X-Ray diffraction (XRD) measurements of the sintered substrates were performed on an Empyrean third Gen. (Malvern

TABLE 4 | Silhouette images at sphere temperature T_S, hemisphere temperature T_H, and at the end of the heating microscopy trial.

Niobium in Air	Niobium in Nitrogen	Tantalum in Air	Tantalum in Nitrogen
			
T_S = 800 °C	T_S = 814°C	T_S = 825 °C	T_S = 804 °C
		Not available	
T_H = 995°C	T_H= 991°C	Not reached	T_H = 993 °C
			
θ ≅ 80°	θ ≅ 45°	θ ≅ 110°	θ ≅ 55°

PANalytical) using a copper x-ray tube with U = 40 kV and I = 40 mA in θ–θ geometry.

All sintered substrates but $Na_2Nb_4O_{11}$ were investigated in the heating microscope at a rate of 10 K/min up to approx. 50°C below decomposition temperature or until reaching the flow point. Due to its low decomposition temperature (see Figure 1), $Na_2Nb_4O_{11}$ was investigated only up to 1000°C.

2.4 | Subsequent Investigation

For selected substrates, namely those on which no wetting and sticking occurred and from which the glass beads could therefore be removed, the surface underneath the glass bead was examined after the heating microscopy trial using XRD. For comparison, an XRD measurement was performed close to the edge of the substrate, which had no contact with the glass.

Certain substrates on which wetting and spreading of the glass melt took place were prepared by means of metallographic cross-sectioning and polishing. A subsequent imaging using a scanning electron microscope (Zeiss GeminiSEM) and energy dispersive spectroscopy (EDS) measurements was performed.

3 | Results

3.1 | Metallic Tantalum and Niobium

DGG X glass formed a high contact angle on both metallic niobium and tantalum when investigated up to 1200°C in air, while somewhat lower contact angles were observed in a nitrogen atmosphere. Table 4 shows silhouette images and temperatures at sphere temperature T_S and hemisphere temperature T_H according to DIN 51730, and the silhouette images and contact angles at the end of the trial.

Both substrates showed pronounced oxidation during the trial. Having a high Pilling–Bedworth–Ratio ratio R_{PB}

$$R_{PB} = \frac{V_{ox}}{n \cdot V_{me}} \quad (1)$$

where V is the molar volume and n the number of metal atoms per oxide molecule, tantalum and niobium tend to form non-protective oxide layers with a high tendency to chip off, explaining the thick, partly cracked, white oxide layer which could be observed after the trial (compare Figure 3).

FIGURE 3 | Photographs of substrate and glass after the heating microscopic trial for tantalum (left) and niobium (right).

It is interesting to note that the contact angle measured under a nitrogen atmosphere, where oxidation of the substrate could be strongly reduced, is lower compared to the result in air, suggesting the oxidation of the substrate hinders wetting and sticking of the glass melt. This contradicts the typically pronounced wetting of other oxides and possibly requires further investigation.

3.2 | Oxides

As can be expected from the results under air and nitrogen, both pure tantalum and niobium oxide substrates showed yet higher contact angles of around 130°. The contact angle was maintained even after an isothermal phase of 3 h at 1000°C and was assumed to be in an equilibrium state. Figure 4 shows the measured contact angle over time.

Figure 5 shows images of the substrate and glass bead after the trial, as well as the silhouette images taken at the beginning of the isothermal stage, after 90 min, and at the end of the trial. The glass droplets could be effortlessly separated from the substrate.

These results are in good agreement with prior investigations on the correlation between sticking and wetting behavior done by the authors [18, 19] and allowed an investigation of the interfaces by means of XRD. The results are displayed in Figure 6.

For tantalum oxide, the XRD measurement at the interface below the glass bead showed the formation of $Na_2Ta_4O_{11}$ (see Figure 6a), clearly indicating a reaction of the substrate with sodium from the glass melt. Performing a Rietveld refinement, the phase amounts were determined to be 87.3 wt.% $Na_2Ta_4O_{11}$ and 12.7 wt.% Ta_2O_5. An XRD measurement performed closer to the edge of the substrate showed almost no sodium tantalate and Ta_2O_5 as the main phase (see Figure 6b).

A similar result was found for niobium oxide, which also reacted with sodium from the glass melt. The compounds found at the interface, however, were mainly $Na_{13}Nb_{35}O_{94}$, which lies in the solid solution range of the TTB phase $Na_{1\pm x}Nb_{3\pm x}O_{8\pm 2x}$ (see Figure 1) and a minor amount of $NaNb_{13}O_{33}$. Again, a measurement closer to the substrate's edge showed a much higher amount of Nb_2O_5. The diffractograms measured with the same procedure as for the tantalum substrates are shown in Figure 7.

To check whether the non-wettability persists even at higher temperatures, the measurements were repeated with a heating rate of 10 K/min up to 1400°C. Again, high contact angles could be observed up to a temperature of about 1315°C in the case of Ta_2O_5 and of about 1140°C in the case of Nb_2O_5, while a rapid wetting took place at higher temperatures (see Figure 8)

The glass gob could not be separated from the substrate at the end of the trial to investigate the surface by means of XRD. Instead, cross sections were prepared and studied with SEM-EDS at different spots (see Figure 9). As can be seen in Figure 9, the glass melt penetrated the Ta_2O_5 substrate and an interface reaction took place, forming an approx. 2–10 µm thick layer at the substrate's surface. Interestingly, an EDS analysis of the layer showed a Ca:Na:Ta ratio of 1:2.6:4 (Spot 1) and 1:3.4:5.3 (Spot 2), revealing that the phase formed is not $Na_2Ta_4O_{11}$ but a mixture or solid solution of $NaTaO_3$ and $CaTa_2O_6$. An EDS measurement slightly deeper in the substrate (3) showed a Na:Ta ratio of 1:2.1 and only 0.5 at.% Ca, indicating $Na_2Ta_4O_{11}$ as observed before by XRD. The dashed line shows the interface between the formed $NaTaO_3$ and $Na_2Ta_4O_{11}$ layers.

As the observed $NaTaO_3$ layer was only approx. 2 µm thick at the thinnest point, it was decided to perform additional grazing incidence x-ray diffraction (GIXRD) measurements with a fixed angle $\omega = 2°$ to exclude the formation of this phase in the non-wetting case. With the densities of Ta_2O_5 $\rho = 8.2$ g•cm^{-3} and Nb_2O_5 $\rho = 4.6$ g•cm^{-3} and the mass attenuation coefficients (MAC) of Ta_2O_5 MAC = 136.27 cm^2•g^{-1} and Nb_2O_5 MAC = 107.62 cm^2•g^{-1}, the penetration depths were calculated to $d = 0.7$ µm for the Ta_2O_5 sample and $d = 1.6$ µm for the Nb_2O_5 sample. Ta_2O_5 and Nb_2O_5 substrates of approximately 20 × 20 mm^2 were prepared[1] and heated in contact with a glass cube to 1000°C. Again, after the heat treatment, the glass could be effortlessly removed from the sample. The interface was then studied by means of GIXRD. Neither $NaTaO_3$ nor $NaNbO_3$ could be observed; the phases found were Ta_2O_5 and $Na_2Ta_4O_{11}$, as well as Nb_2O_5 and $Na_{13}Nb_{35}O_{94}$, consistent with the results observed for the heating microscopy samples.

From the results above, it appeared reasonable that the tantalates and niobates formed at the interface are responsible for the non-wetting behavior observed. A change in the interface composition with increased temperature would initiate the wetting process.

3.3 | Tantalates and Niobates

Following the results discussed in Section 3.2, it was decided to synthesize several niobates and tantalates (see Table 3) by means of solid-state reactions as described in Section 2.3 and repeat the thermo-optical trials.

Table 5 shows the silhouette images obtained at the beginning of the isothermal phase at 1000°C, after 90 min, and at the end of the isothermal phase after 3 h. Contact angles comparable to those of DGGX on Nb_2O_5 formed for all niobates. For the tantalates, however, only the TTB phase showed high contact angles, while wetting took place for $Na_2Ta_4O_{11}$ and $NaTaO_3$, and the flow point was reached before the end of the isothermal phase.

Again, the glass beads could be separated from the niobate substrates and examined by means of XRD. Interestingly, all three substrates showed the formation of the TTB-like phase,

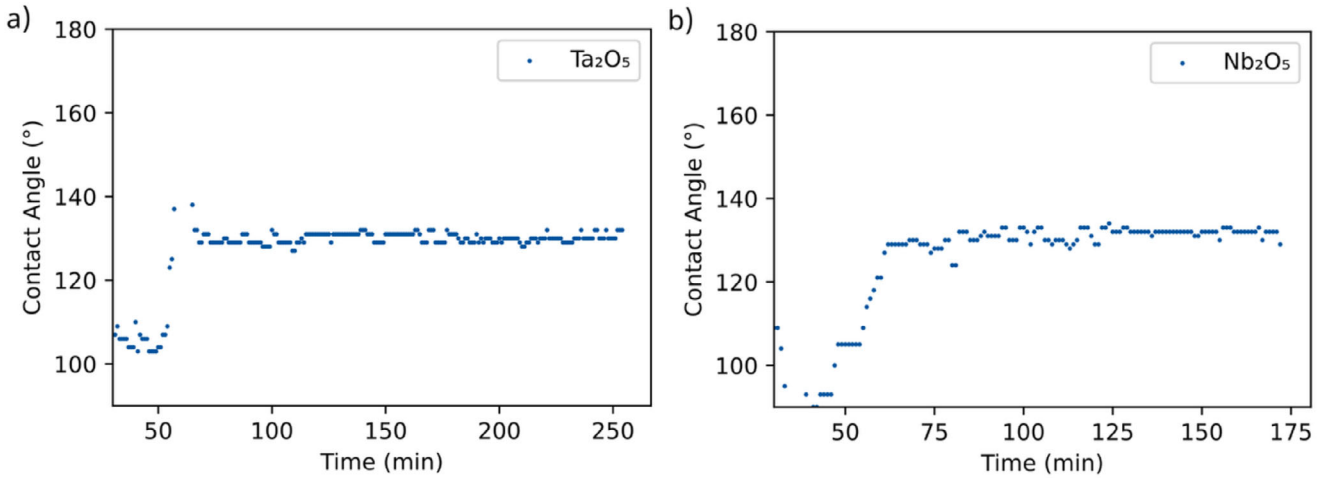

FIGURE 4 | Contact angle of DGG X glass on Ta_2O_5 (a) and Nb_2O_5 (b) during isothermal holding at 1000°C.

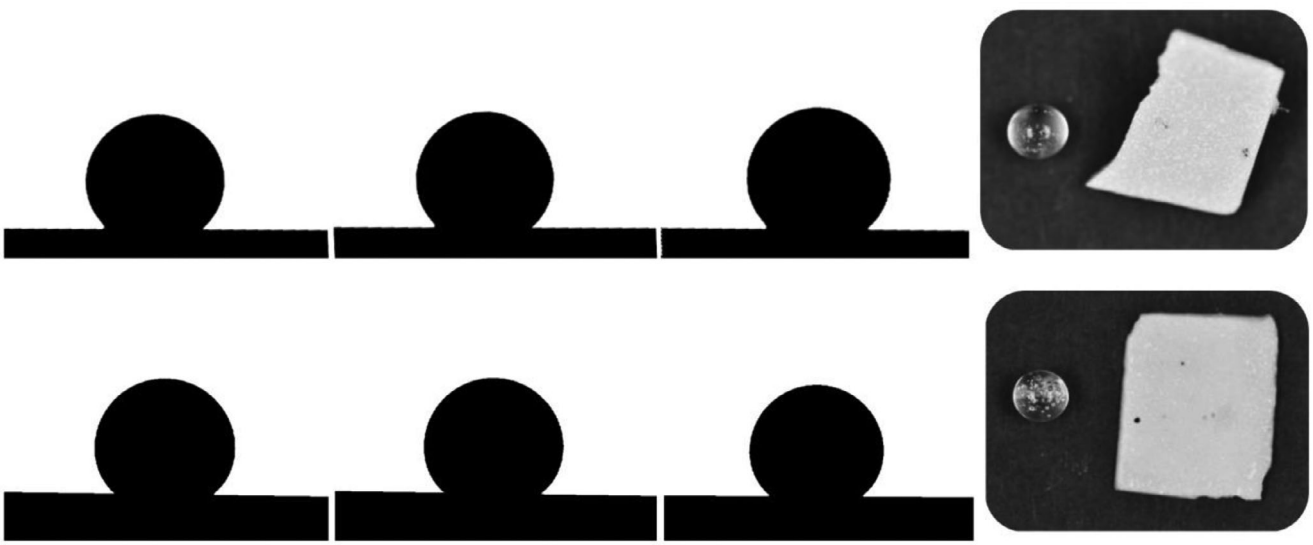

FIGURE 5 | Silhouette images taken at the beginning of the isothermal stage at 1000°C, after 90 min, and at the end of the trial and photography after the trial for tantalum oxide (upper row) and niobium oxide (lower row).

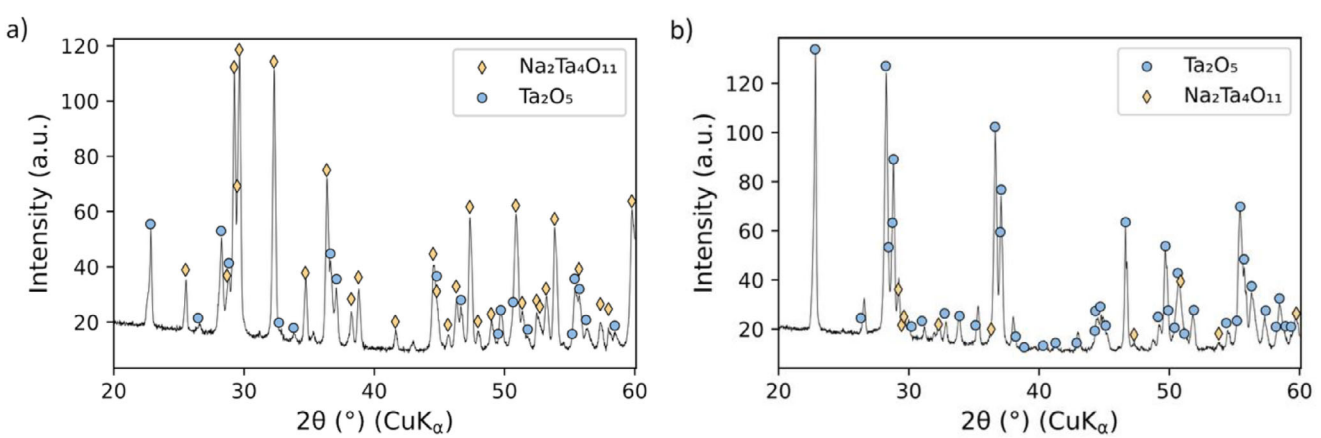

FIGURE 6 | XRD diffractograms of the Ta_2O_5 substrate, measured after the thermo-optical trial below the removed glass drop (a) and close to the substrate's edge (b).

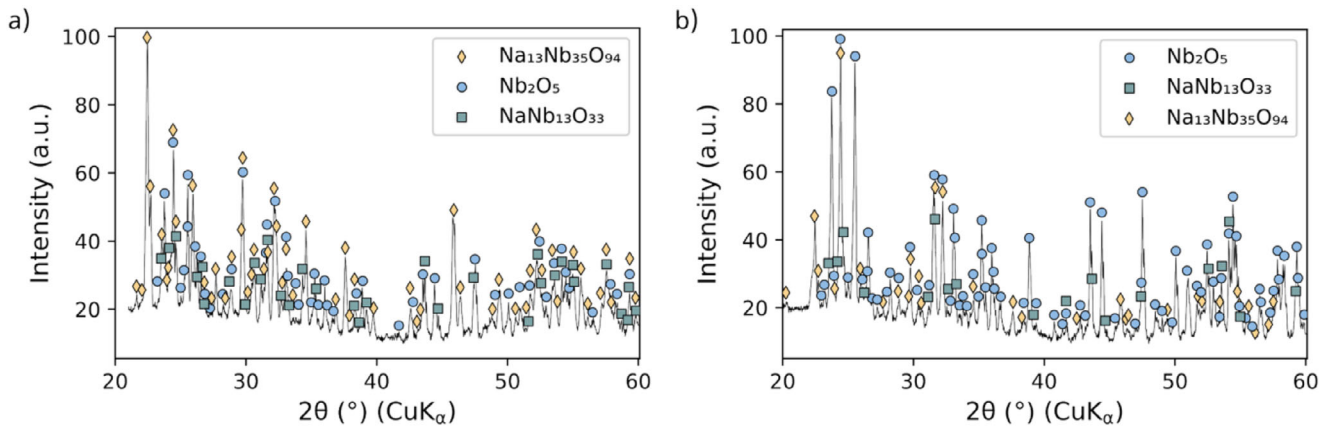

FIGURE 7 | XRD diffractograms of the Nb_2O_5 substrate, measured after the thermo-optical trial below the removed glass drop (a) and close to the substrate's edge (b).

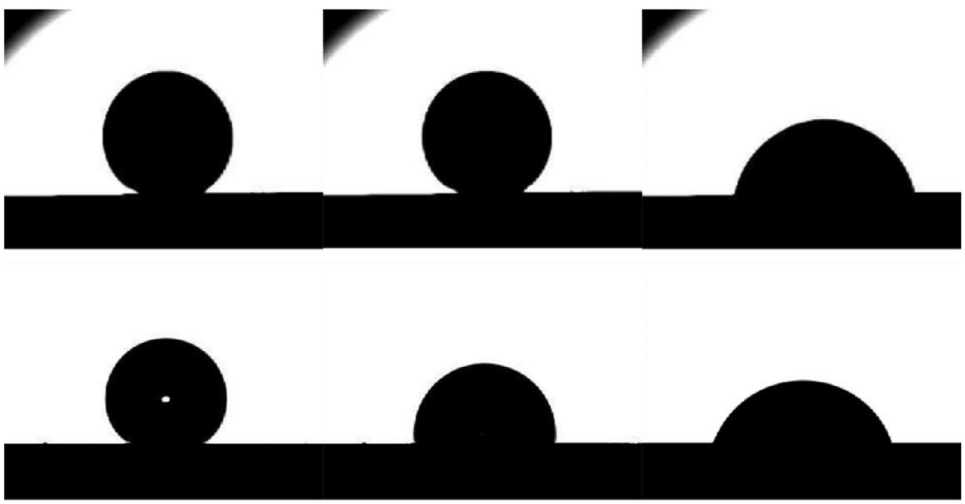

FIGURE 8 | Series of silhouette image showing the spreading of DGGX on Ta_2O_5, taken at 1300°C, 1310°C, and 1320°C (upper row) and on Nb_2O_5 taken at 1130°C, 1150°C, and 1190°C (lower row).

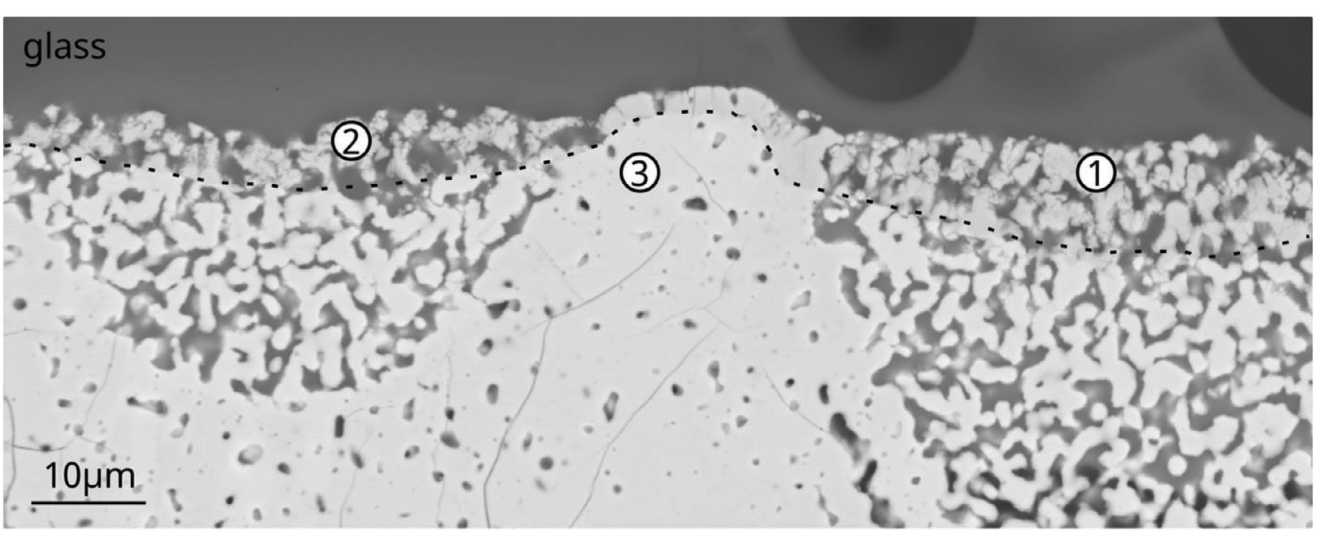

FIGURE 9 | Cross section through the wetted Ta_2O_5 sample with EDS measuring points (1), (2), and (3). A 2–10 µm thick interface layer has formed, indicated by the dashed line.

TABLE 5 | Silhouette images of DGG X on several niobates and tantalates taken at 1000°C, at the beginning of the isothermal phase (left), after 90 min (middle), and at the end of the trial after 3 h (right).

$NaNb_3O_8$			
$Na_2Nb_4O_{11}$	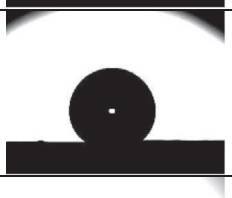	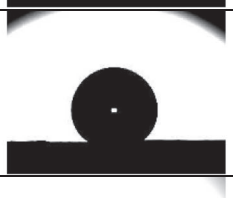	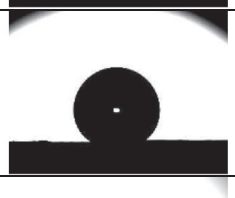
$NaNbO_3$	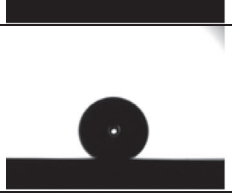	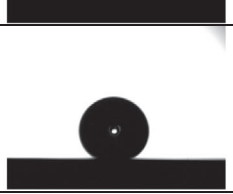	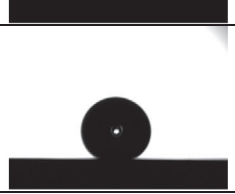
TTB	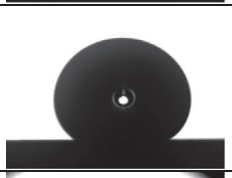	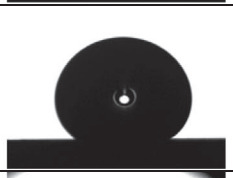	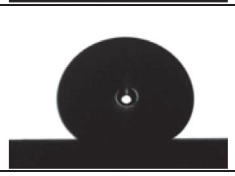
$Na_2Ta_4O_{11}$	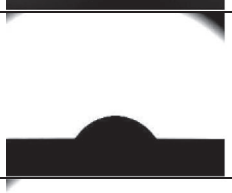		Not available
$NaTaO_3$	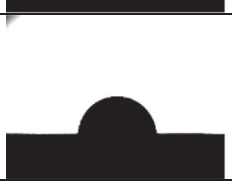		Not available

which could be refined to $Na_{13}Nb_{35}O_{94}$, at the interface below the glass bead. This result indicates that this phase could be crucial to developing non-wetting behavior. Likewise, the TTB-like tantalate showed a high contact angle and non-wetting.

Due to the spreading of the glass melt and sticking to the substrate, an investigation by means of XRD was not useful for $Na_2Ta_4O_{11}$ and $NaTaO_3$. It was decided to perform SEM-EDS measurements instead. The images of the cross-sections are shown in Figure 10.

Both substrates were penetrated by the glass melt. For the $NaTaO_3$ substrate, no layer formation at the interface could be observed (see Figure 10a), like in the case of Ta_2O_5. EDS measurements close to the interface (Spot 1) and deeper in the substrate (Spot 2) showed no significant difference in sodium content, with the calculated theoretical composition being $Na_{1.0}Ta_{1.1}O_{2.9}$ (1) and $Na_{1.0}Ta_{1.0}O_{2.9}$ (2). In the case of the $Na_2Ta_4O_{11}$ substrate, however, the formation of a second phase close to the interface could be observed (see Figure 10b). In the highlighted area in Figure 10b, the interface between those two layers becomes particularly visible. The calculated composition of this phase was $Ca_{0.1}Na_{0.8}Ta_{1.1}O_3$ (Spot 3), again revealing the formation of $NaTaO_3$ and $CaTa_2O_6$ at the interface. Slightly deeper in the substrate, the calculated composition was $Na_{2.0}Ta_{4.5}O_{11.3}$ (Spot 4).

The results above clearly suggest that the formation of TTB phases is essential for non-wettability, while the formation of the perovskite-like 1:1 phases seems to enhance wettability. The results obtained on Ta_2O_5 allow the conclusion that the presence of the 1:2 phase alone does not lead to wetting. However, it remains debatable why $NaTaO_3$ forms at the interface of the $Na_2Ta_4O_{11}$ substrate at lower temperatures than on Ta_2O_5. One explanation could be that the visually observed more porous character of the prepared $Na_2Ta_4O_{11}$ sample compared to the denser Ta_2O_5 substrate enhances the reaction. On the other hand, $KTaO_3$ obtained by solid-state reactions was observed to form in a two-step process with the intermediate formation of $K_2Ta_4O_{11}$ in the literature before [20]. The same two-step reaction path is feasible for the formation of $NaTaO_3$. After the formation of $Na_2Ta_4O_{11}$, however, the Na-depleted glass melt near the interface with Ta_2O_5 may not offer enough Na to promote a reaction to the 1:1 phase at low temperatures. At the same time, the TTB phase, which forms in niobates, cannot be formed on the substrates $Na_2Ta_4O_{11}$ and $NaTaO_3$, as it is only stable at temperatures above 1200°C.

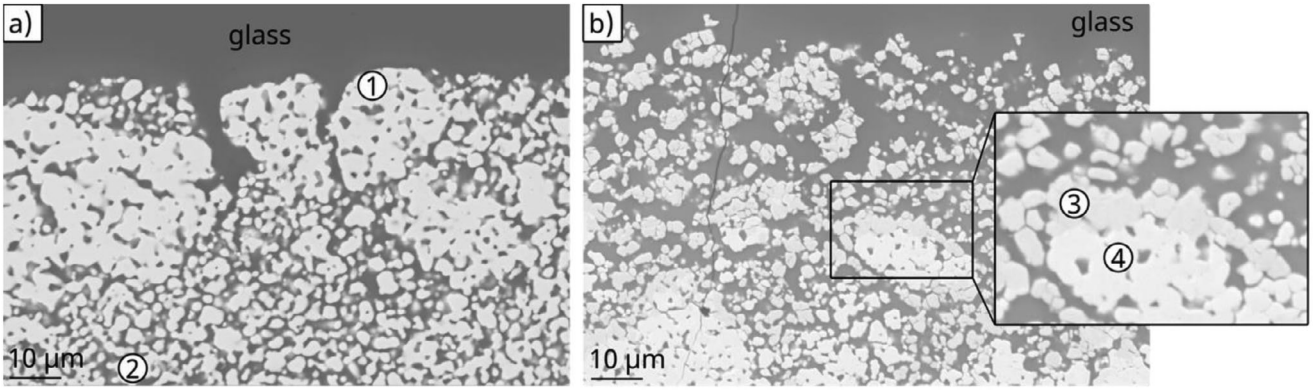

FIGURE 10 | Cross section through the wetted $NaTaO_3$ sample (a) with EDS measurement Spots (1) and (2) and $Na_2Ta_4O_{11}$ sample (b) with EDS measurement Spots (3) and (4).

4 | Conclusion

The wetting and sticking behavior of a soda lime silicate glass was investigated for tantalum, niobium, their oxides, and various tantalates and niobates. Remarkably high contact angles were found whenever oxidation and the formation of specific tantalates or niobates occurred. Especially the formation of TTB-like phases and potentially $Na_2Ta_4O_{11}$ and $Na_2Nb_4O_{11}$ seems to promote non-wettability. This finding could be especially important for developing alternative glass contact materials that are stable in an oxidizing atmosphere. Ongoing investigations, therefore, shall assess the implementation in non-sticking coatings.

In future work, a molecular dynamics simulation of the contact between glass and an energetically optimized substrate surface, as well as an analysis of the interaction mechanisms based on the obtained binding states, binding mechanisms, and interatomic potentials, shall be performed. Quantum chemical and molecular dynamic approaches will be combined to identify the crucial influencing factors on an atomic basis and to validate the experimental findings. The authors hope that this will provide a comprehensive explanation for the unusual wetting behavior observed.

Acknowledgments

The authors wish to thank Philipp Jacobs for conducting the XRD measurements.

Open access funding enabled and organized by Projekt DEAL.

Funding

Funded by the Deutsche Forschungsgemeinschaft (DFG, German Research Foundation) — 512796744.

Conflicts of Interest

The authors declare no conflicts of interest.

Data Availability Statement

Data from the results presented can be provided upon request.

Endnote

[1] The preparation of larger samples instead of using the original heating microscopy samples, enabled GIXRD measurements with a larger spot size of approx. 10 mm, which reduces the measurement duration to an appropriate level.

References

1. V. Gurylev, "A Review on the Development and Advancement of Ta_2O_5 as a Promising Photocatalyst," *Materials Today Sustainability* 18 (March 2022): 100131, https://doi.org/10.1016/j.mtsust.2022.100131.

2. C. Chaneliere, J. L. Autran, R. A. B. Devine, and B. Balland, "Tantalum Pentoxide (Ta_2O_5) Thin Films for Advanced Dielectric Applications," *Materials Science and Engineering R Reports* 22, no. 6 (May 1998): 269–322, https://doi.org/10.1016/s0927-796x(97)00023-5.

3. I. Abuetwirat and T. Palai-Dany, "Dielectric Properties of Niobium Oxide Film and Tantalum Oxide Film at Electrolytic Niobium and Tantalum Capacitors," in *2012 ELEKTRO* (IEEE, May 2012), 484–487, https://doi.org/10.1109/elektro.2012.6225671.

4. M. Soltanalipour and J. Khalil-Allafi, "Exploring the Role of Tantalum and Its Coatings in Medicine: Insights Into Biological Performance and Innovative Developments," *Transactions of the IMF* 103, no. 5 (August 2025): 264–271, https://doi.org/10.1080/00202967.2025.2536428.

5. G. Mohandas, N. Oskolkov, M. McMahon, P. Walczak, and M. Janowski, "Porous Tantalum and Tantalum Oxide Nanoparticles for Regenerative Medicine," *Acta Neurobiologiae Experimentalis* 74, no. 2 (June 2014): 188–196, https://doi.org/10.55782/ane-2014-1984.

6. Y.-Y. Chang, H.-L. Huang, H.-J. Chen, C.-H. Lai, and C.-Y. Wen, "Antibacterial Properties and Cytocompatibility of Tantalum Oxide Coatings," *Surface and Coatings Technology* 259 (April 2014): 193–198, https://doi.org/10.1016/j.surfcoat.2014.03.061.

7. M. S. Safavi, F. C. Walsh, L. Visai, and J. Khalil-Allafi, "Progress in Niobium Oxide-Containing Coatings for Biomedical Applications: A Critical Review," *ACS Omega* 7, no. 11 (March 2022): 9088–9107, https://doi.org/10.1021/acsomega.2c00440.

8. V. V. Starikov, S. L. Starikova, A. G. Mamalis, S. N. Lavrynenko, and J. J. Ramsden, "The Application of Niobium and Tantalum Oxides for Implant Surface Passivation," *Journal of Biological Physics and Chemistry* 7, no. 4 (December 2007): 65–68, https://doi.org/10.4024/40704.jbpc.07.04.

9. R. S. Roth, H. S. Parker, W. S. Brower, and J. L. Waring, "Phase Equilibriums, Crystal Chemistry, and Crystal Growth of Alkali Oxide-Metal Oxide Systems," in *Fast Ion Transport in Solids, Solid State Batteries and Devices, Proceedings of the NATO Advanced Study Institute*, ed. W. Van Gool (North-Holland Publishing Company, September 1972), 217–232.

10. E. Irle, R. Blachnik, and B. Gather, "The Phase Diagrams of Na_2O and K_2O With Nb_2O_5 and the Ternary System Nb_2O_5-Na_2O-Yb_2O_3," *Thermochimica Acta* 179 (April 1991): 157–169, https://doi.org/10.1016/0040-6031(91)80344-i.

11. B. J. Kennedy, A. K. Prodjosantoso, and C. J. Howard, "Powder Neutron Diffraction Study of the High Temperature Phase Transitions in $NaTaO_3$," *Journal of Physics Condensed Matter* 11, no. 33 (August 1999): 6319–6327, https://doi.org/10.1088/0953-8984/11/33/302.

12. S. K. Mishra, R. Mittal, V. Y. Pomjakushin, and S. L. Chaplot, "Phase Stability and Structural Temperature Dependence in Sodium Niobate: A High-Resolution Powder Neutron Diffraction Study," *Physical Review B* 83, no. 13 (April 2011), 134105–134109, https://doi.org/10.1103/physrevb.83.134105.

13. C. N. W. Darlington and K. S. Knight, "High-Temperature Phases of $NaNbO_3$ and $NaTaO_3$," *Acta Crystallographica Section B Structural Science* 55, no. 1 (February 1999): 24–30, https://doi.org/10.1107/s010876819800963x.

14. T. S. Ercit, F. C. Hawthorne, and P. Černý, "The Crystal Structure of Synthetic Natrotantite," *Bulletin De Minéralogie* 108, no. 3 (January 1985): 541–549, https://doi.org/10.3406/bulmi.1985.7848.

15. N. Masó, D. I. Woodward, A. Várez, and A. R. West, "Polymorphism, Structural Characterisation and Electrical Properties of $Na_2Nb_4O_{11}$," *Journal of Materials Chemistry* 21, no. 32 (January 2011): 12096, https://doi.org/10.1039/c1jm11848j.

16. W. J. Zhang, W. Liu, and H. Y. Shen, "Second-Harmonic Generation Transition in $NaNb_3O_8$ Solid Solutions," *Applied Physics Letters* 58, no. 21 (May 1991): 2334–2335, https://doi.org/10.1063/1.104913.

17. R. Nedjar, M. M. Borel, A. Leclaire, and B. Raveau, "The Sodium Niobate $NaNb_3O_8$: A Novel Lamellar Oxide Synthesized by Soft Chemistry," *Journal of Solid State Chemistry* 71, no. 1 (November 1987): 182–188, https://doi.org/10.1016/0022-4596(87)90157-5.

18. C. Roos, J.-H. Veltmaat, and P. Jacobs, "A New Model for Describing the Glass to Metal Interaction in Forming," *Glass Europe* 2 (November 2024): 137–149, https://doi.org/10.52825/glass-europe.v2i.976.

19. P. Engelmann and C. Roos, "Thermo-Optical Set-Up to Investigate Non-Isothermal Glass-Metal Contact," *Glass Europe* 3 (October 2025): 195–202, https://doi.org/10.52825/glass-europe.v3i.2866.

20. A. Axelsson, Y. Pan, M. Valant, and N. Alford, "Synthesis, Sintering, and Microwave Dielectric Properties of $KTaO_3$ Ceramics," *Journal of the American Ceramic Society* 92, no. 8 (August 2009): 1773–1778, https://doi.org/10.1111/j.1551-2916.2009.03130.x.